Supplementary materials

Magnetic properties of 3D lanthanide complexes with 1,3-bis(diphenylphosphoryl)-2-oxapropane: The slow magnetic relaxation of Yb(III) compounds

Serafima S. Slobodskaia[a,*], Nikolay N. Efimov[b], Alina S. Galkina[b], Galina S. Tsebrikova[a], Andrey B. Ilyukhin[b], Irina S. Ivanova[b], Vladimir E. Baulin[c], Aslan Yu. Tsivadze[a]

[a] *Frumkin Institute of Physical Chemistry and Electrochemistry, Russian Academy of Sciences, Leninskii pr. 31/4, Moscow, 119071 Russia*

[b] *Kurnakov Institute of General and Inorganic Chemistry, Russian Academy of Sciences, Leninskii pr. 31, Moscow, 119991 Russia*

[c] *Institute of Physiologically Active Compounds, Federal Research Center for Problems of Chemical Physics and Medicinal Chemistry, Russian Academy of Sciences, Severnyi proezd 1, Moscow region, Chernogolovka, 142432 Russia*

** e-mail: SlobodskayaSi@yandex.ru*

Table S1. The results of the C, H, N-analysis of **1**–**7**

Compound	Type of the result	C, %	H, %	N, %
$[Dy_2L_3(NO_3)_6]_n \cdot 8.1nH_2O$ (**1**)	Exp., (%):	42.94	4.06	3.92
	Theor., (%):	42.92	4.04	3.85
$[Lu_2L_3(NO_3)_6]_n \cdot 6nH_2O$ (**2**)*	Exp., (%):	43.52	3.82	4.04
	Theor., (%):	43.17	3.87	3.87
$[Y_2L_3(NO_3)_6]_n \cdot 8.64nH_2O$ (**3**)	Exp., (%)::	46.26	4.47	4.26
	Theor., (%):	45.81	4.35	4.11
$[(Dy_{0.07}Lu_{0.93})_2L_3(NO_3)_6]_n \cdot 3.48nH_2O$ (**4**)	Exp., (%):	44.05	3.71	4.28
	Theor., (%):	44.13	3.72	3.96
$[(Dy_{0.03}Y_{0.97})_2L_3(NO_3)_6]_n \cdot 7.68nH_2O$ (**5**)	Exp., (%):	46.27	4.28	4.41
	Theor., (%):	46.14	4.21	4.14
$[Yb_2L_3(NO_3)_6]_n \cdot 6nH_2O$ (**6**)	Exp., (%):	43.10	3.92	3.86
	Theor., (%):	43.25	3.88	3.88
$[(Yb_{0.16}Y_{0.84})_2L_3(NO_3)_6]_n \cdot 7.62nH_2O$ (**7**)	Exp., (%):	45.69	4.21	4.00
	Theor., (%):	45.59	4.25	4.09

* Composition of the complex is given according to elemental analysis and XRD patterns

Table S2. Basic crystallographic data and structure refinement results for complexes **1**, **3-7**.

Compound	**1**	**3**	**4**	**5_100K**	**5_250K**	**6**
Formula	$C_{78}H_{88.2}Dy_2N_6O_{35.1}P_6$	$C_{78}H_{89.28}N_6O_{35.64}P_6Y_2$	$C_{78}H_{78.96}Dy_{0.14}Lu_{1.86}N_6O_{30.48}P_6$	$C_{78}H_{87.36}Dy_{0.06}N_6O_{34.68}P_6Y_{1.94}$		$C_{78}H_{84}N_6O_{33}P_6Yb_2$
M	2182.16	2044.71	2122.12	2029.54	2029.54	2165.41
T, K	143(2)	100(2)	100(2)	100(2)	250(2)	100(2)
Wavelength,λ, Å	0.71073	0.71073	0.71073	0.71073	0.71073	0.71073
Crystal system	Cubic	Cubic	Cubic	Cubic	Cubic	Cubic
Space group.	I-43d	I-43d	I-43d	I-43d	I-43d	I-43d
a, Å	26.5290(4)	26.5165(11)	26.2405(13)	26.4345(11)	26.650(5)	26.2926(10)
V, Å^3	18670.8(8)	18644(2)	18068(3)	18472(2)	18927(11)	18176(2)
Z	8	8	8	8	8	8
D_x, *g/cm*^{3}	1.553	1.457	1.560	1.460	1.424	1.583
μ, mm^{-1}	1.777	1.428	2.323	1.450	1.415	2.236
F(000)	8808	8419	8513	8339	8339	8704
Sample size, mm	0.24 x 0.20 x 0.18	0.32 x 0.28 x 0.16	0.24 x 0.24 x 0.24	0.32 x 0.28 x 0.16	0.32 x 0.28 x 0.16	0.24 x 0.20 x 0.12
θ range, deg	2.171, 32.034	2.172, 28.307	2.195, 28.306	2.436, 30.507	2.417, 28.226	2.191, 30.499
h, *k*, *l* ranges	-38<=h<=39	-35<=h<=35	-34<=h<=34	-37<=h<=37	-35<=h<=35	-37<=h<=37
	-39<=k<=39	-35<=k<=35	-34<=k<=34	-37<=k<=37	-35<=k<=35	-37<=k<=37
	-39<=l<=39	-35<=l<=35	-34<=l<=34	-37<=l<=37	-35<=l<=35	-37<=l<=37
Number of measured reflections	108944	140277	150620	178307	158956	149030
Number of independent reflections, R_{int}	5433, 0.0381	3850, 0.0493	3763, 0.0619	4722, 0.0793	3911, 0.0723	4637, 0.0545
Completeness up to θ = 25.24°	99.9 %	99.8 %	99.9 %	99.8 %	99.9 %	99.9 %
Absorption correction	Semi-empirical from equivalents	Semi-empirical from equivalents	Semi-empirical from equivalents	Semi-empirical from equivalents	Semi-empirical from equivalents	Semi-empirical from equivalents
Max, min of transmission	0.7463, 0.6392	0.7454, 0.569	0.4311, 0.3132	0.7461, 0.6446	0.7457, 0.6377	0.7461, 0.6653
Refinement method	Full-matrix least-squares on F^2	Full-matrix least-squares on F^2	Full-matrix least-squares on F^2	Full-matrix least-squares on F^2	Full-matrix least-squares on F^2	Full-matrix least-squares on F^2
Number of parameters	5433 / 0 / 209	3850 / 0 / 204	3763 / 0 / 192	4722 / 0 / 204	3911 / 0 / 204	4637 / 0 / 200
S	0.990	0.996	1.082	1.132	1.102	0.900
*R*1, *wR*2 [*I*>2σ(*I*)]	0.0167, 0.0437	0.0234, 0.0725	0.0198, 0.0544	0.0259, 0.0599	0.0261, 0.0607	0.0158, 0.0453
*R*1, *wR*2 (all data)	0.0195, 0.0452	0.0249, 0.0734	0.0246, 0.0599	0.0283, 0.0608	0.0304, 0.0626	0.0183, 0.0468
Flack parameter	-0.0218(19)	-0.0046(18)	-0.030(3)	-0.0209(15)	-0.0237(18)	-0.017(2)
$\Delta\rho_{max}/\Delta\rho_{min}$ e/Å^3	0.281, -0.368	0.417, -0.178	0.453, -0.278	0.308, -0.305	0.195, -0.194	0.520, -0.740
CCDC	2357217	2357221	2403597	2403595	2403596	2357220

Compound	**7**
Formula	$C_{78}H_{87.24}N_6O_{34.62}P_6Y_{1.68}Yb_{0.32}$
M	2053.25
T, K	100(2)
Wavelength,λ, Å	0.71073
Crystal system	Cubic
Space group.	I-43d
a, Å	26.5250(16)
V, Å^3	18662(3)
Z	8
D_x, *g/cm*^{3}	1.462
μ, mm^{-1}	1.546
F(000)	8417
Sample size, mm	0.20 x 0.10 x 0.09
θ range, deg	2.428, 25.039
h, *k*, *l* ranges	-31<=h<=29
	-26<=k<=31
	-31<=l<=31
Number of measured reflections	41923
Number of independent reflections, R_{int}	2762, 0.0792
Completeness up to θ = 25.24°	99.8 %
Absorption correction	Semi-empirical from equivalents
Max, min of transmission	0.874, 0.748
Refinement method	Full-matrix least-squares on F^2
Number of parameters	2762 / 0 / 200
S	1.121
*R*1, *wR*2 [*I*>2σ(*I*)]	0.0332, 0.0819
*R*1, *wR*2 (all data)	0.0359, 0.0830
Flack parameter	-0.018(3)
$\Delta\rho_{max}/\Delta\rho_{min}$ e/Å^3	0.609, -0.347
CCDC	2434794

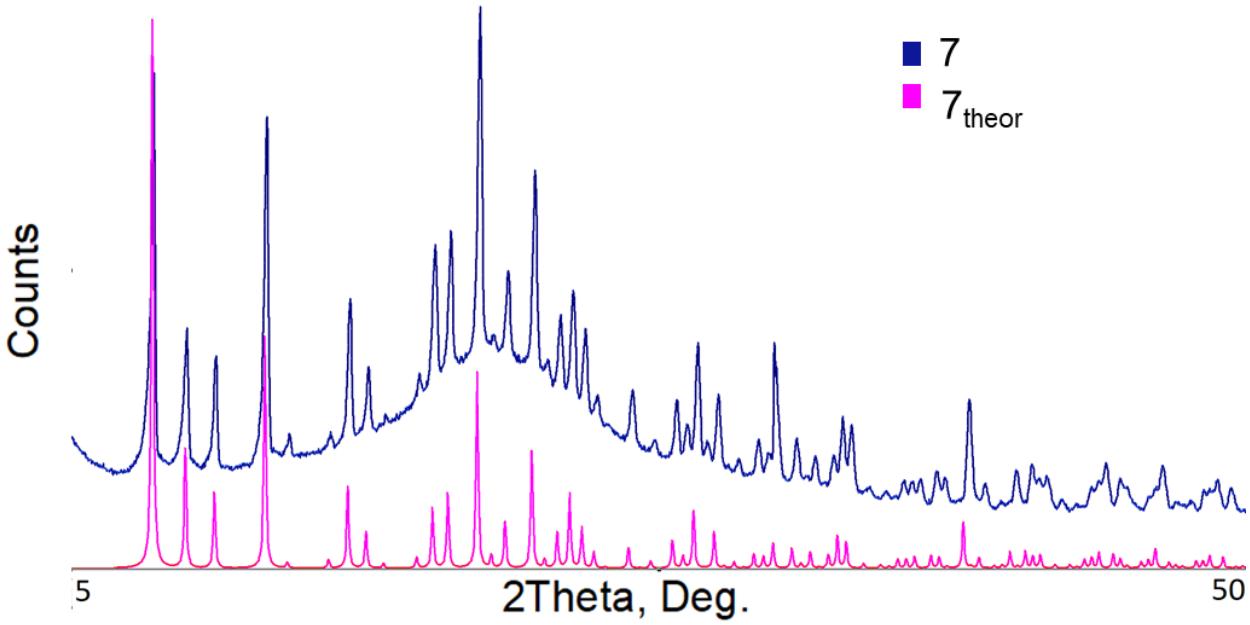

Fig. S1 X-ray patterns of compound **7**

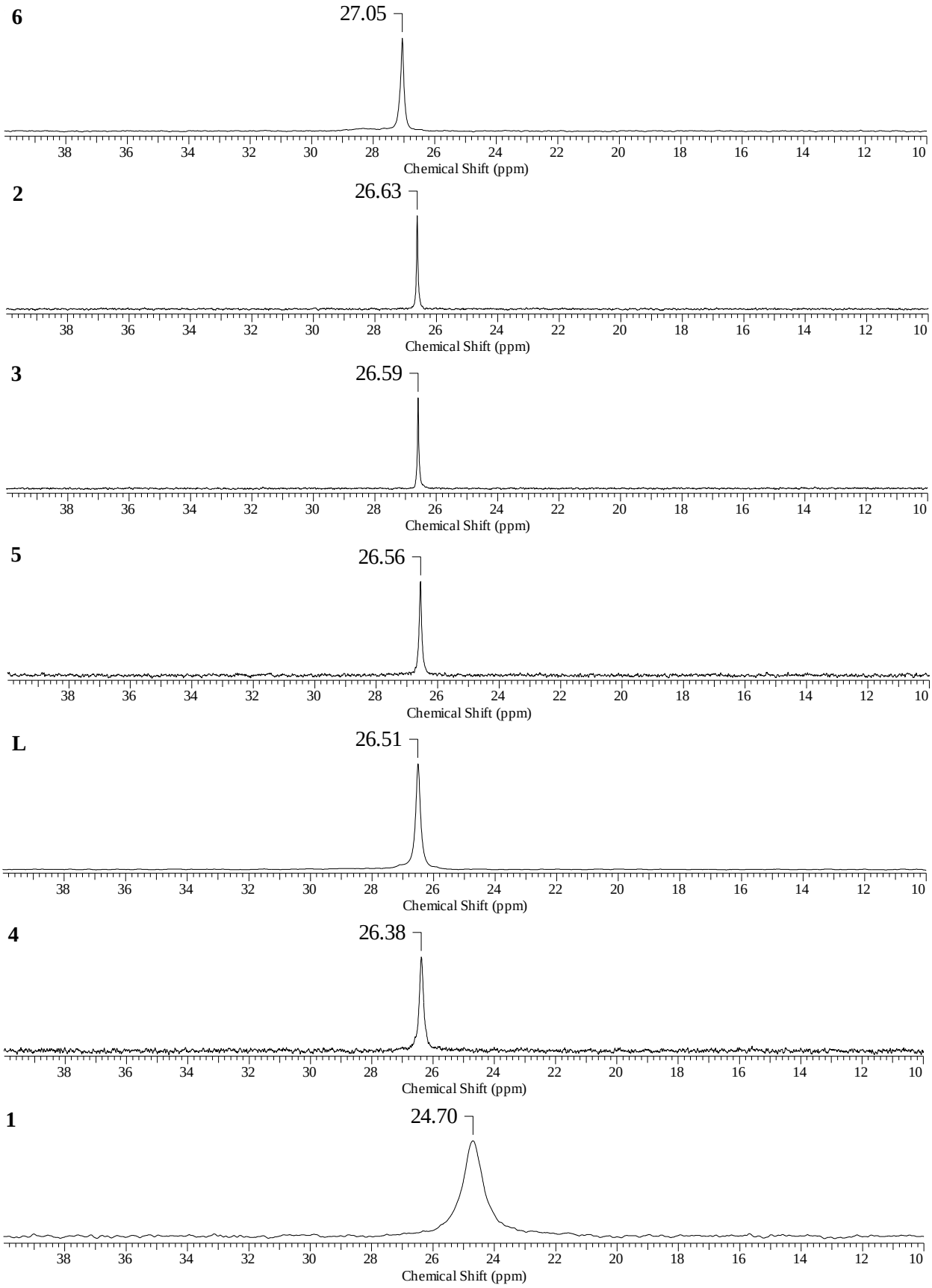

Fig. S2 ^{31}P NMR spectra of ligand L and its complexes in DMSO-d_6

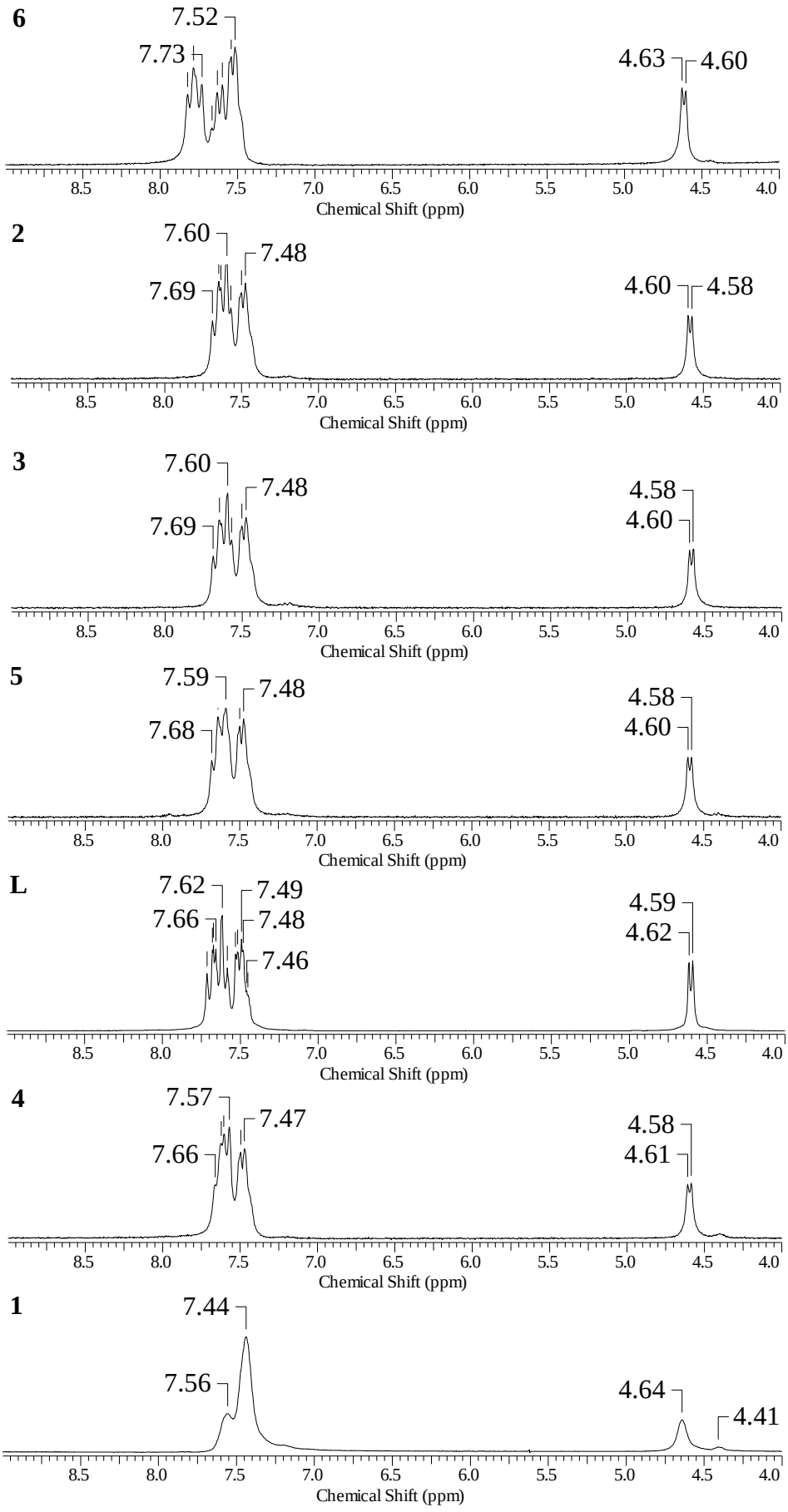

Fig. S3 ^{1}H NMR spectra of ligand L and its complexes in DMSO-d_6

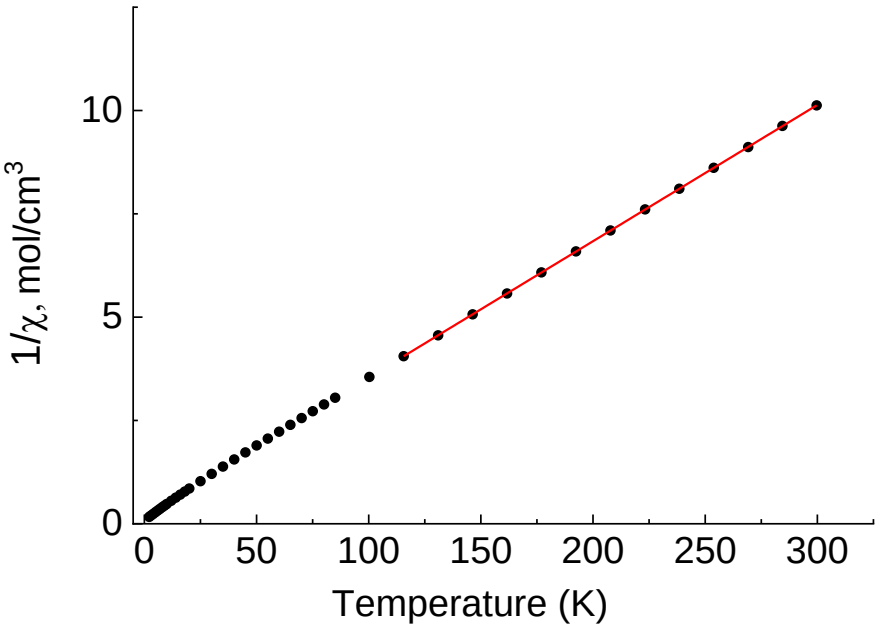

Fig. S4 Dependence of the inverse magnetic susceptibility on the temperature for **1** (H_{dc} = 5000 Oe). The red line is the approximation of the Curie-Weiss law

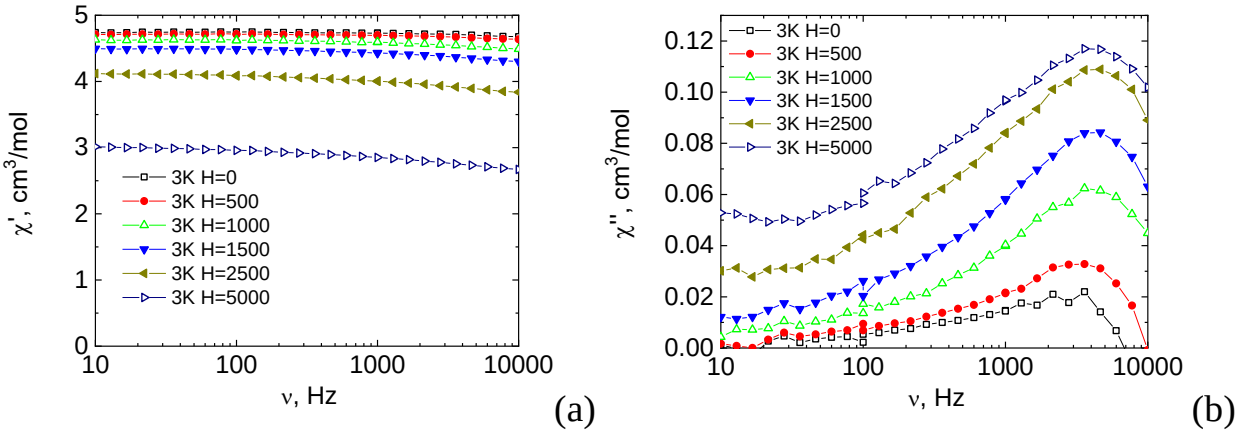

Fig. S5 Frequency dependencies of the real χ' (a) and imaginary χ'' (b) components of the ac susceptibility for **1** at 3 K in various magnetic fields (0–5000 Oe). Solid lines are visual guides

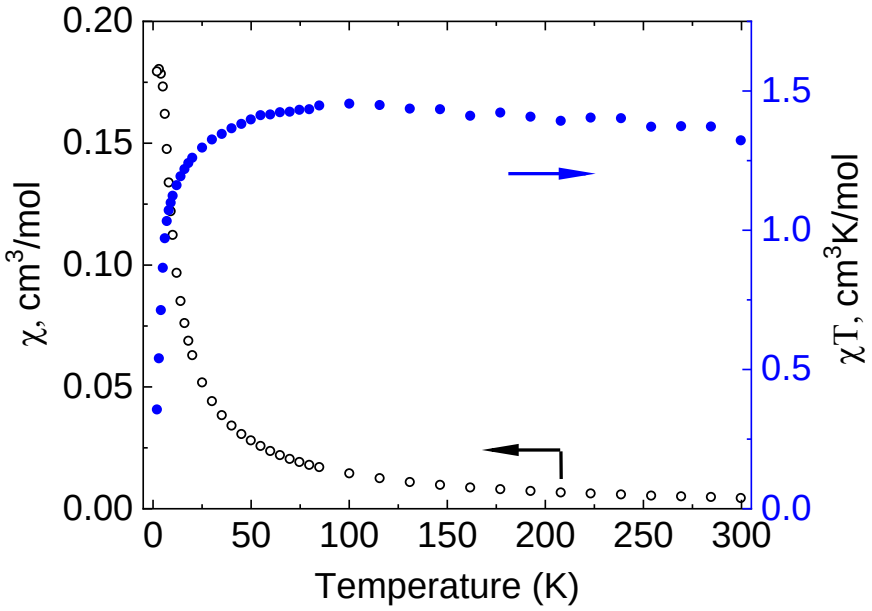

Fig. S6 Temperature dependencies of magnetic susceptibility (•) and χT (■) for **4** (H_{dc} = 5000 Oe)

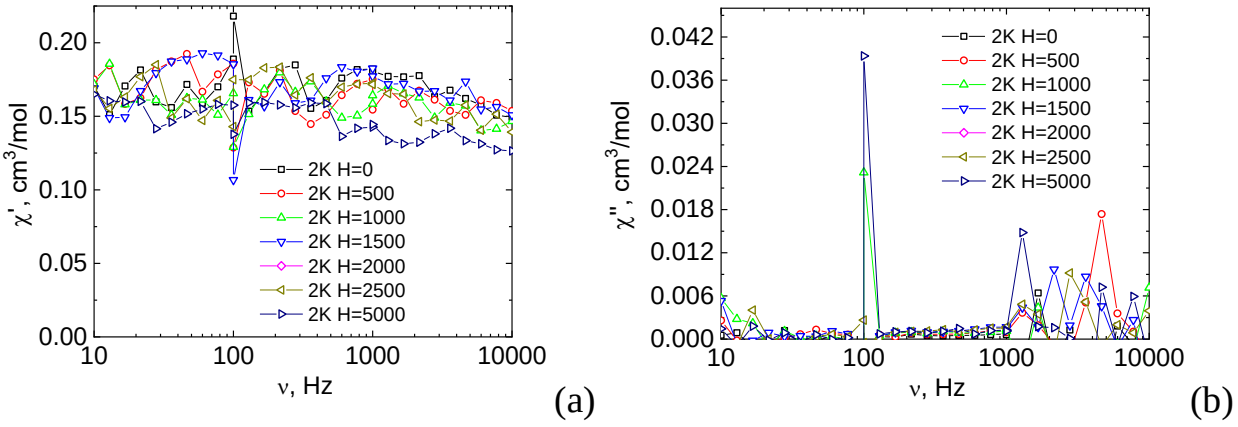

Fig. S7 Frequency dependencies of the real χ' (a) and imaginary χ'' (b) components of the ac susceptibility for **4** at 2 K in various magnetic fields (0 – 5000 Oe). Solid lines are visual guides

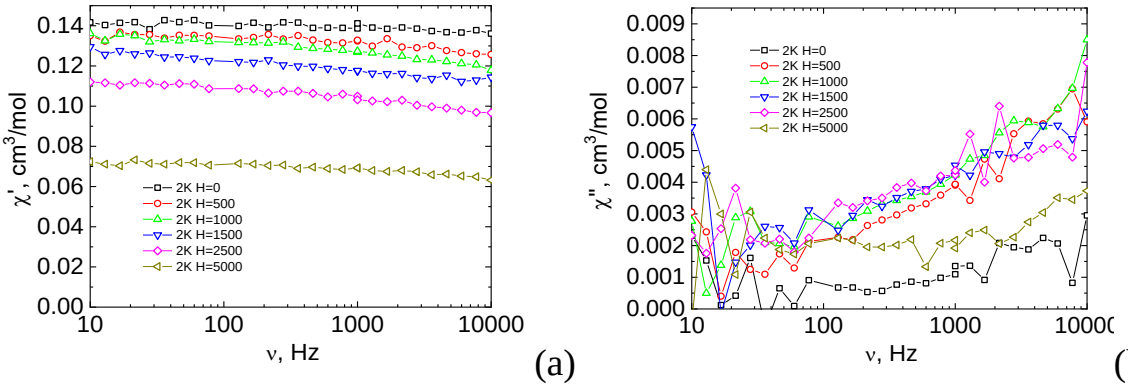

Fig. S8 Frequency dependencies of the real χ' (a) and imaginary χ'' (b) components of the ac susceptibility for **5** at 2 K in various magnetic fields (0 – 5000 Oe). Solid lines are visual guides

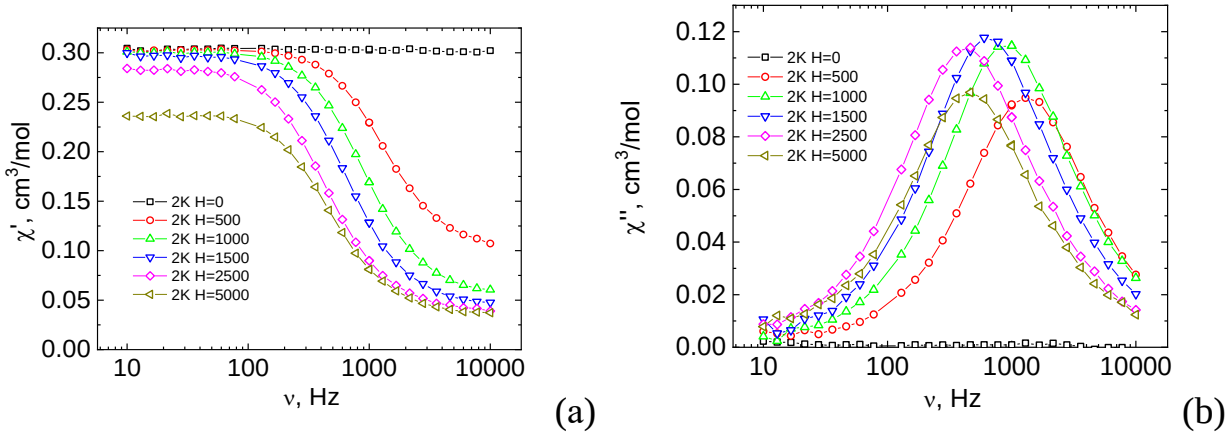

Fig. S9 Frequency dependencies of the real χ' (a) and imaginary χ'' (b) components of the ac susceptibility for **6** at 2 K in various magnetic fields (0 – 5000 Oe). Solid lines are visual guides

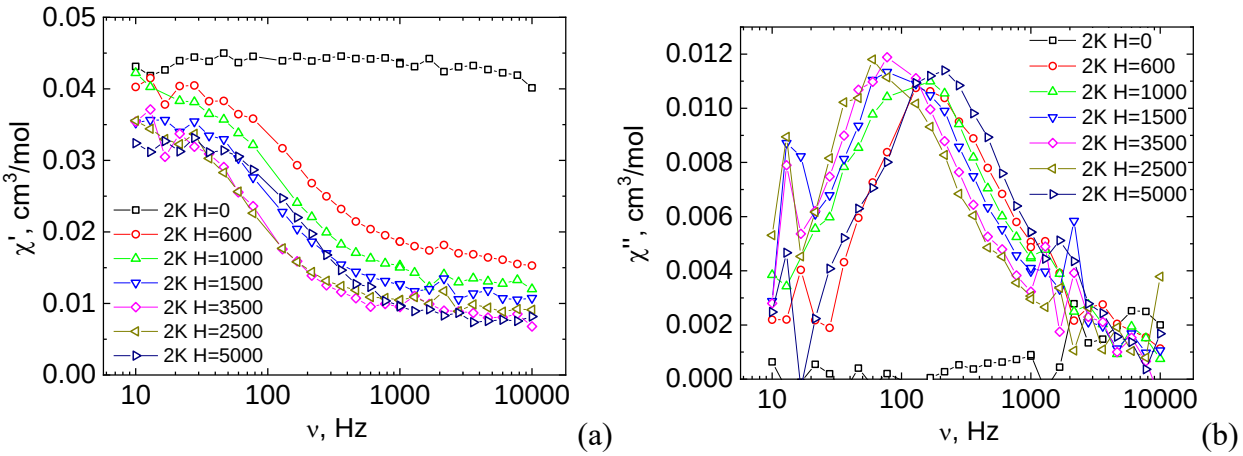

Fig. S10 Frequency dependencies of the real χ' (a) and imaginary χ'' (b) components of the ac susceptibility for **7** at 2 K in various magnetic fields (0 – 5000 Oe). Solid lines are visual guides

Table S3. Fitting of the *τ vs. T* dependencies for **6**

Dependence of the relaxation time τ on the reciprocal temperature for complex **6** (*H* = 2500 Oe, *T* = 2-3.6 K).	Fit function, temperature range, and the best-fit parameters with uncertainties.
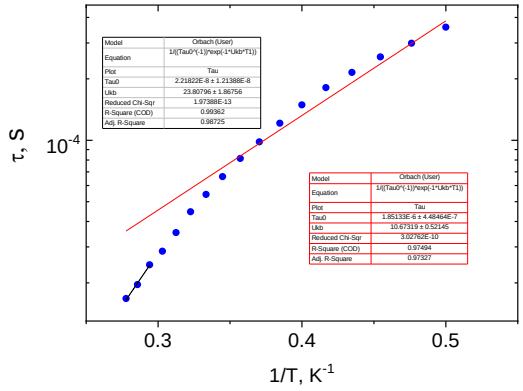	**Orbach** $\tau = \tau_0 \cdot \exp(\Delta E/kT)$ T = 3.4-3.6 K $\Delta E/k$ = 24 ± 2 K $\tau_0 = 2 \cdot 10^{-8} \pm 1 \cdot 10^{-8}$ s R^2 = 0.99362 (black line) T = 2.0-3.6 K $\Delta E/k$ =10.7 ± 0.5 K $\tau_0 = 1.9 \cdot 10^{-6} \pm 0.4 \cdot 10^{-6}$ s R^2 = 0.97494 (red line) *Unsatisfactory fit*

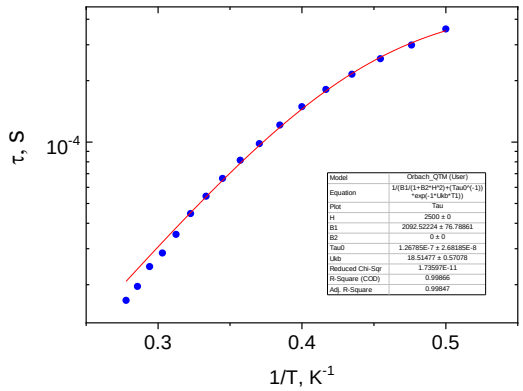	**Orbach+ QTM** $\tau^{-1} = \tau_0^{-1}\cdot\exp(-\Delta E/kT)+ B$ $\Delta E/k$ = 18.5 ± 0.6 K $\tau_0 = 1.3\cdot10^{-7} \pm 0.3\cdot10^{-7}$ s B= 2093 ± 77 s^{-1} R^2 = 0.99866
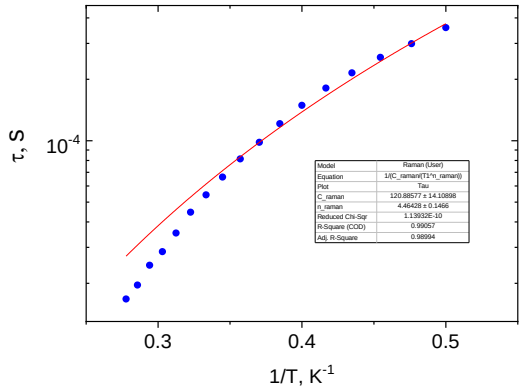	**Raman** $\tau^{-1} = C_{\text{Raman}}T^{\text{n\_Raman}}$ C_{Raman}=121 ± 14 $s^{-1}K^{-\text{nRaman}}$ n_{Raman}=4.46 ± 0.15 R^2 = 0.99057
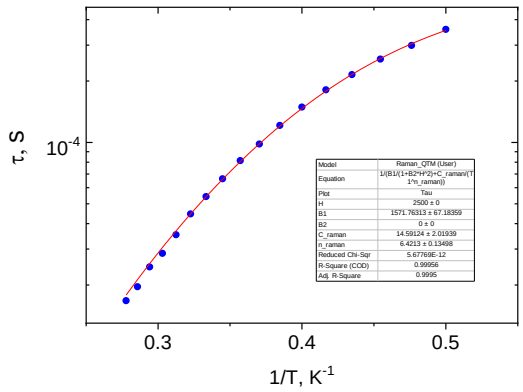	**Raman+ QTM** $\tau^{-1} = C_{\text{Raman}}T^{\text{nRaman}} + B$ C_{Raman}= 15 ± 2 $s^{-1}K^{-\text{nRaman}}$ n_{Raman}= 6.4 ± 0.1 B = 1572 ± 67 s^{-1} R^2 = 0.99956
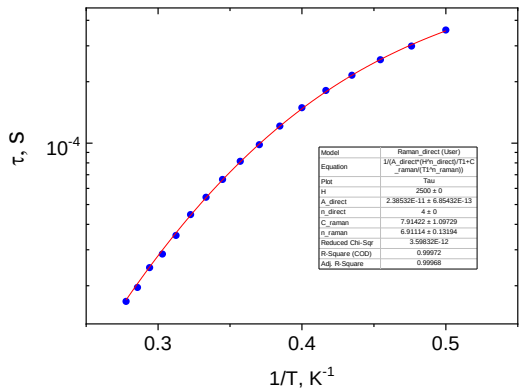	**Raman+Direct** $\tau^{-1} = C_{\text{Raman}}T^{\text{nRaman}} + A_{direct}TH^4$ C_{Raman}= 8 ± 1 $s^{-1}K^{-\text{nRaman}}$ n_{Raman}=6.9 ± 0.1 A_{direct} = $2.39\cdot10^{-11}$ ± $0.07\cdot10^{-11}$ $K^{-1}Oe^{-4}s^{-1}$ R^2 = 0.99972

<table>
<tr>
<td> 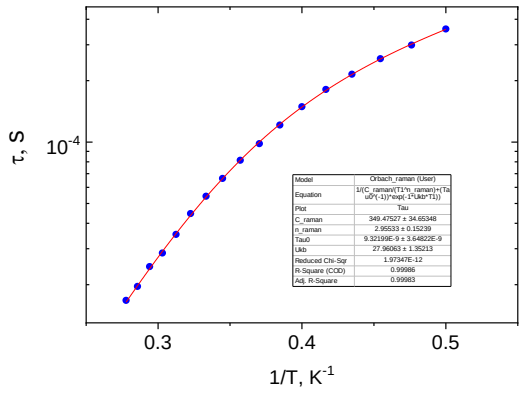
</td>
<td>Orbach+Raman
$\tau^{-1} = \tau_0^{-1}\cdot\exp(-\Delta E/kT)+C_{\text{Raman}}T^{\text{nRaman}}$

$\Delta E/k$ = 28 ± 1 K
τ_0 =9·10^{-9} ± 4·10^{-9} s
C_{Raman}= 349 ± 35 s^{-1}K$^{-\text{nRaman}}$
n_{Raman}= 3.0 ± 0.2
R^2 = 0.99986</td>
</tr>
<tr>
<td> 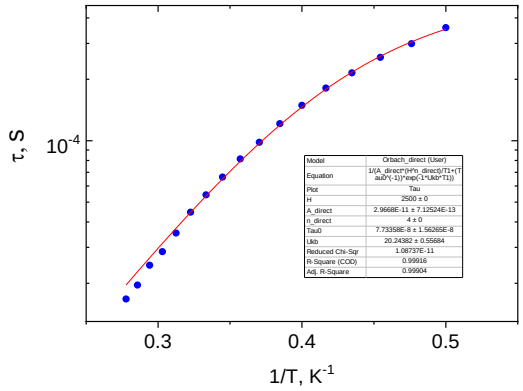
</td>
<td>Orbach+Direct
$\tau^{-1} = \tau_0^{-1}\cdot\exp(-\Delta E/kT)+A_{direct}TH^4$

$\Delta E/k$ = 20.2 ± 0.6 K
τ_0 = 8·10^{-8} ± 2·10^{-8}s
A_{direct} = 2.97·10^{-11} ± 0.07·10^{-11} K^{-1}Oe^{-4}s^{-1}
R^2 = 0.99916</td>
</tr>
<tr>
<td> 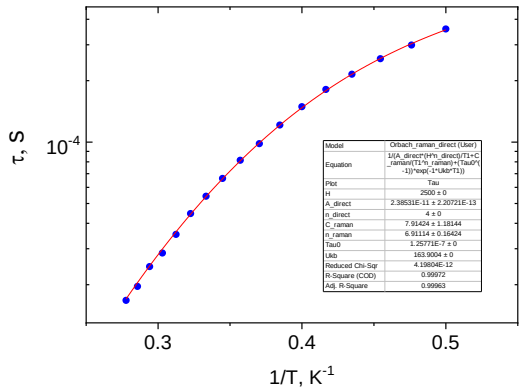
</td>
<td>Orbach+Raman+Direct
$\tau^{-1} = \tau_0^{-1}\cdot\exp(-\Delta E/kT)+C_{\text{Raman}}T^{\text{nRaman}}$
$+A_{direct}TH^4$

$\Delta E/k$ = 164 ±0 K
τ_0 = 1.26·10^{-7} ± 0s
C_{Raman}= 8 ± 1 s^{-1}K$^{-\text{nRaman}}$
n_{Raman}= 6.9±0.2
A_{direct} = 2.39·10^{-11} ± 0.02·10^{-11} K^{-1}Oe^{-4}s^{-1}
R^2 = 0.99972
Overparameterization</td>
</tr>
<tr>
<td> 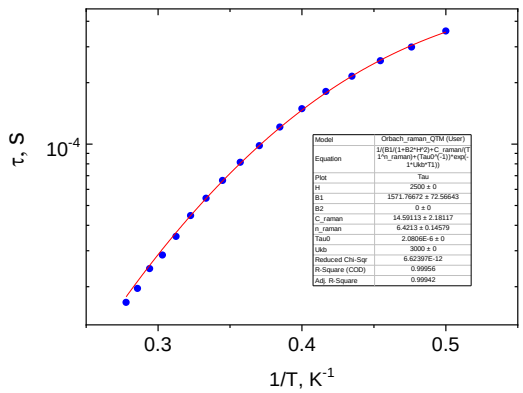
</td>
<td>Orbach+Raman+QTM
$\tau^{-1} = \tau_0^{-1}\cdot\exp(-\Delta E/kT)+C_{\text{Raman}}T^{\text{nRaman}}$
$+B$

$\Delta E/k$ = 3000 ± 0.0 K
τ_0 = 2·10^{-6} ± 0 s
C_{Raman}= 15 ± 2 s^{-1}K$^{-\text{nRaman}}$
n_{Raman}= 6.42 ± 0.15
B = 1572 ± 73 s^{-1}
R^2 = 0.99956
Overparameterization</td>
</tr>
</table>